Discover Oncology

Research

Effects of albumin-bound paclitaxel combined with *Sophora subprostrate* polysaccharide on inflammatory factors and immune function in breast cancer rats

Changli Ding[1] · Zhuolin Li[2] · Ying Zheng[1] · Kaichun Li[1] · Wenyan Yu[1] · Lingzhijie Kong[1] · Zhiyong Zhang[1]

Received: 20 November 2024 / Accepted: 30 April 2025
Published online: 10 May 2025
© The Author(s) 2025 OPEN

Abstract

Background Tumor occurrence and growth are highly correlated with the degree of inflammation and immunological activity. Reducing the level of inflammation in tumor-bearing body to relieve immune suppression and enhance anti-tumor immune function has become an important strategy for tumor treatment.

Objective To investigate the effect of albumin-bound paclitaxel combined with *Sophora subprostrate* polysaccharide (SSP) on inhibiting inflammation, reducing immunosuppression, enhancing anti-tumor immune function and slowing the progression of tumor in tumor-bearing rats, and to provide certain scientific basis for the clinical application of combined drugs in tumor.

Methods The rats were put into three groups at random: normal control, model group, and drug treatment group. After the end of drug intervention, the tumor was taken out and weighed to observe the tumor growth of the rats. Tumor necrosis factor (TNF-α), interleukin (IL) 1β, IL-10, perforin, and granzyme B were found by Western blot in the local tumor tissues of experimental rats. The protein expression levels of Arginase-1 (Arg-1) and Cyclooxygenase 2 (COX-2) were determined. HE staining was used to observe the inflammatory infiltration of the tumor. Using flow cytometry, the proportions of anti-tumor immune cells—CD8 + T cells, NK cells, and immunosuppressive cells—in local tumor tissues were evaluated. In addition, spleen T cells isolated from normal rats were co-cultured with spleen myeloid derived suppressor cells (MDSC) from tumor-bearing rats in the model group and the combined treatment group. Cell Trace Far Red was used to identify T cell proliferation, flow cytometry was used to determine the level of T cell activation from CD25 expression, and in vivo immunosuppression in tumor-bearing rats was examined.

Results The combined therapy group experienced a considerable decrease in tumor weight as compared to the model group. TNF-α and IL-1p levels in the vicinity of the tumor tissues reduced following intervention, although IL-10 levels, which are anti-inflammatory cytokines, did not significantly change. The results of the HE staining revealed that the intervention group's tumor had less inflammatory infiltration than the model group did. After intervention, the percentages of CD8 + T cells and NK cells in local tumor tissues increased. Additionally, the intervention group's levels of protein expression for perforin and granzyme B were considerably higher than those of the model group. In the nearby tumor tissues, there were lots of MDSC. Following the intervention, the proportion of MDSC in the local tumor tissues

[$] Changli Ding and Zhuolin Li are the Co-first author.

Supplementary Information The online version contains supplementary material available at https://doi.org/10.1007/s12672-025-02539-7.

✉ Zhiyong Zhang, zhiyongzhang4r60@163.com | [1]Department of Oncology, Shanghai Fourth People's Hospital Affiliated to Tongji University, 1279 Sanmen Road, Hongkou District, Shanghai, China. [2]Department of Oncology, Wuhan Central Hospital, Tongji Medical College, Huazhong University of Science and Technology, Wuhan, China.

was significantly reduced, and the expansion of MDSC was reduced. Additionally, the intervention group's COX-2 and Arg-1 protein expression levels in the tumor-specific tissues were significantly lower than those of the model group. The outcomes of in vitro co-culture demonstrated that rats in the combination group had higher levels of T cell proliferation and activation than animals in the model group.

Conclusions Albumin-bound paclitaxel combined with Sophora subprostrate polysaccharide can reduce the local inflammation level, promote the proportion of CDB + T cells and NK cells and cell killing function, reduce the proportion of MDSC and immunosuppressive level, enhance the anti-tumor immune function of tumor-bearing mice, and slow the growth of tumors.

Keywords Albumin-bound paclitaxel · Sophora subprostrate polysaccharide · Breast cancer · Immunity · Inflammatory factors

1 Introduction

Breast cancer is a malignant tumor originating from the epithelial cells of the breast, and its incidence has been steadily increasing, with a concerning trend of younger age at diagnosis in recent years [1]. This rise is attributed to a variety of factors, including environmental exposures, genetic predisposition, age, lifestyle, and dietary habits [2]. Environmental pollutants, endocrine disruptors, and sedentary behavior are among the lifestyle factors that have been implicated in gene mutations that contribute to the development of breast cancer. Moreover, with the ongoing process of industrial modernization and urbanization, the incidence of breast cancer in many developing countries has shown a marked increase, a phenomenon that warrants urgent public health attention. Despite advances in early detection and treatment, the overall prognosis for advanced breast cancer remains poor, highlighting the need for innovative therapeutic alternatives aimed at improving survival outcomes and quality of life for affected individuals.

Recent studies have illuminated the crucial role of inflammation in the pathogenesis and progression of breast cancer. Chronic inflammation is recognized as a significant risk factor for various cancers, including breast cancer, and is closely linked to tumor initiation, growth, and metastasis [3–5]. Inflammatory cytokines such as interleukin-1β (IL-1β) [6, 7], tumor necrosis factor-alpha (TNF-α) [8], and interleukin-6 (IL-6) [9] have been identified as key mediators of this process, facilitating tumor progression and resistance to therapies [10–12]. Furthermore, inflammatory processes within the tumor microenvironment are known to impair the effectiveness of both chemotherapy and immunotherapy [13, 14], exacerbating the challenge of treating advanced cancer. Emerging evidence suggests that inflammation not only supports tumorigenesis but also contributes to immune evasion, creating an immunosuppressive microenvironment that favors tumor growth [15]. In particular, myeloid-derived suppressor cells (MDSCs), which accumulate in response to inflammatory signals, have been shown to play a pivotal role in this immune suppression. MDSCs inhibit the proliferation, migration, and activation of natural killer (NK) cells [16–18] and CD8 + T cells [19], which are essential for the body's anti-tumor immune response, thus facilitating immune escape and reducing the efficacy of treatments [20, 21].

The mechanistic insights into MDSC-induced immunosuppression highlight several critical pathways that could be targeted for therapeutic intervention [22]. For instance, MDSCs impair T cell activation by consuming essential amino acids, inhibiting the synthesis of key molecules involved in T cell receptor (TCR) signaling, and by producing enzymes that block TCR activation [23, 24]. Additionally, MDSCs modulate the NK cell function by upregulating inhibitory receptors and downregulating activating receptors, further suppressing the immune response [25]. Moreover, MDSCs induce the production of other immunosuppressive cells, such as regulatory T cells (Tregs) and tumor-associated macrophages (TAMs), which further exacerbate the immunosuppressive tumor microenvironment [26]. This intricate interplay between inflammation, immune cells, and tumor cells creates a vicious cycle that not only facilitates tumor growth but also hinders the efficacy of current immunotherapies. A growing body of research suggests that MDSCs are found in various cancers, including breast, lung, and liver cancers, and their accumulation correlates with disease progression and poor prognosis [27–29]. Given the central role of MDSCs in tumor immunosuppression, targeting these cells or the inflammatory pathways that drive their accumulation could provide a promising therapeutic approach to enhance anti-tumor immunity and improve treatment outcomes.

However, current treatments that aim to reduce inflammation and modulate the immune response, such as anti-inflammatory drugs, often come with significant side effects and off-target effects [30, 31], limiting their clinical applicability in cancer treatment. Therefore, exploring novel combination therapies that can target both the inflammatory

pathways and the tumor itself is an important direction for future research. One promising candidate is albumin-bound paclitaxel (Nab-PTX), a new form of paclitaxel that is conjugated with human serum albumin to enhance its targeting and tissue distribution within tumors. Nab-PTX has been shown to improve paclitaxel's pharmacokinetics and reduce toxicity, making it an effective treatment for metastatic breast cancer, particularly for patients who have developed resistance to standard chemotherapy [32]. The FDA and CFDA have approved Nab-PTX for the treatment of metastatic breast cancer, underscoring its clinical significance. In addition to Nab-PTX, the potential role of natural compounds, such as those derived from traditional Chinese medicine, is gaining increasing attention in cancer therapy. For example, Sophora subprostrate, a plant with a long history of use in traditional Chinese medicine, has shown anti-inflammatory and anti-tumor properties, particularly through its polysaccharide constituents. Although much of the research on Sophora subprostrate has focused on its alkaloids, its polysaccharides remain relatively underexplored. Recent studies suggest that combining Sophora subprostrate polysaccharides with conventional therapies like Nab-PTX could enhance therapeutic efficacy by modulating the immune microenvironment and reducing inflammation, providing a multi-faceted approach to cancer treatment.

In conclusion, while significant strides have been made in understanding the inflammatory and immune mechanisms underlying breast cancer progression, much remains to be explored in terms of effectively targeting these pathways to improve treatment outcomes. Further investigation into the synergistic effects of combination therapies, particularly those that modulate inflammation and immune response, holds great promise in the fight against breast cancer. By addressing the challenges of immune evasion and inflammation within the tumor microenvironment, new therapeutic strategies can be developed to improve survival rates and the quality of life for breast cancer patients.

2 Materials and methods

2.1 Experimental animals

The Beijing Weitong Lihua Laboratory Animal Technology Co., LTD. provided healthy female wild type rats, aged 6 to 8 weeks, which were maintained in the animal room of the Institute of Acupuncture and Moxibustion, China Academy of Chinese Medical Sciences. With 3–4 rats per cage and unrestricted access to food and water, the mice were fed in cages at a room temperature of 22–25 °C. Experimental manipulation was initiated after one week of adaptive feeding. Control and experimental groups were randomized to ensure that no systematic bias influenced the results. The inclusion criteria for animal selection included no visible signs of disease or deformities.

2.2 Cell lines

The rat SHZ-88 breast cancer cell line, which was purchased from the ATCC Cell Bank (catalog number CRL-2323), was used to induce breast cancer in the experimental animals. SHZ-88 cells were chosen due to their well-documented characteristics as a model for breast cancer research. These cells were cultured under standard conditions in a humidified incubator at 37 °C with 5% CO_2.

2.3 Establishment of breast cancer model

SHZ-88 cells were seeded. Trypsin (Sigma, T3924) was used to break down the cells into single cell suspension, and the digestion was stopped by adding the proper amount of warmed medium containing 100% FBS (Thermo Fisher, 26140-079). The cells were then transferred to a 15 mL centrifuge tube and centrifuged (290 g, 5 min, 4 °C), with the supernatant discarded and resuspended in 1 mL warmed PBS (Thermo Fisher, 14190-094). To determine cell viability and number, 10 µL of the cell suspension was combined with µL of trypan blue (Thermo Fisher, 15250061). After uniform staining, 10 µL was aspirated and applied to the cell counting plate, which was then placed in an automatic cell counter. Cells with viability higher than 98% were used for the preparation of animal models. The original cell suspension was diluted into a single cell suspension at a concentration of 1×10^6 cells/mL using PBS, depending on the number of viable cells.

The skin around the right second breast pad and armpit was exposed. 0.1 mL cell suspension (1×10^5 cells) was aspirated from a 1 mL syringe and injected subcutaneously into the second breast pad on the right side of rats. At the same location, 0.1 mL of PBS was injected into the rats in the control group. The animals were put back in the food box after

the vaccination, and frequent tumor formation observations were made. Those with poor tumor formation or uniformity in the same time were excluded, and the tumor size was about 50 mm3, which was regarded as successful modeling.

2.4 Experimental groups

The rats were randomly divided into the following groups: EA Group: Treatment with experimental agents (Sophora subprostrate polysaccharide, albumin-bound paclitaxel). Model Group: Tumor-induced rats without any treatment. Control Group: Rats injected with PBS only. For the EA Group, the combined treatment of albumin-bound paclitaxel (Abraxane, BMS-184,474) and Sophora subprostrate polysaccharide was administered. The dosage of albumin-bound paclitaxel was determined based on previous studies and adjusted for the weight of the rats, with a typical dose of 20 mg/kg body weight, administered intraperitoneally once every 3 days. Sophora subprostrate polysaccharide was administered at a dose of 100 mg/kg body weight, delivered orally once daily. The Model Group consisted of rats that underwent the same tumor induction procedure but received no therapeutic intervention, allowing for the observation of tumor progression without treatment. The Control Group received only PBS injections to account for any effects of the injection process itself, ensuring that the observed results were specifically due to the treatments in the EA Group.

2.5 Weight of tumor

Taking the tumor volume change as the index, when the tumor volume of the EA group and the model group showed statistical difference for the first time, the samples were taken after another four days of observation. Solid tumors and spleens of rats in each group were removed, weighed, recorded and photographed.

2.6 MTT assay

The cells were cultivated in an incubator at 37 °C with 5% CO_2 and seeded in 96-well cell culture plates at 8000 cells/well. Each well of the control wells received 100 µL of cell suspension, while each well of the blank wells received 100 µL of culture media. Following a 24-h culture period, each well received a series of 100 µL additions of Sophora subprostrate polysaccharide and albumin-bound paclitaxel in PBS solution, 50 µL additions of Sophora subprostrate polysaccharide and albumin-bound paclitaxel in PBS solution for the combination group, and 100 µL additions of PBS for the blank and control wells. Each well received 20 µL of MTT solution (Sigma, M5655) after 48 h of culture, and then it was put in the incubator for an additional 4 h of cultivation. After that, the supernatant was aspirated, and the 96-well plate was inverted on filter paper to blot out the residual solvent. To completely dissolve the purple crystals, 150 µL more of DMSO (Sigma, D8418) was added to each well and agitated for 10 min. Utilizing a microplate reader, the absorbance at a wavelength of 490 nm was measured to calculate the amount of cell inhibition. CompuSyn software developed by Chou-Talalay calculation method [20] was used to calculate IC50 and combination index according to the inhibition rate of cells at different drug concentrations. When $CI = 1$, the effect was additive, and when $CI < 1$, the effect was synergistic. $CI > 1$ denotes hostility [21].

2.7 HE staining

The animals were subjected to deep anesthesia by intraperitoneal injection of 10% chloral hydrate solution (Sigma, C1054). The fixative solution of 4% paraformaldehyde ((Sigma, 158127), approximately 20 mL) was then infused into the circulating blood after the 0.9% sodium chloride solution had flushed it out through the heart. Local tumor tissues were removed and stored in fixative solution. A gradient of alcohol from low to high concentration was used for the transparent treatment. After paraffin embedding, 5 µm thick section specimens were prepared, placed on slides of glass, and placed on a 45° C baking machine for 5 min.

The prepared section specimens were deparaffinized, rinsed with tap water, and then placed in hematoxylin staining solution for 5 min. After washing the excess staining solution, the specimens were placed in 1% hydrochloric acid ethanol for 1–3 s to differentiate, and then blue was returned in 0.2% ammonia water for 1–2 s. After rinsing with tap water, the nucleus and cytoplasm staining could be observed under the microscope. Then dehydrated and transparent with gradient ethanol. The slides were sealed with neutral gum after blow drying, looked at under a microscope, and taken pictures for examination.

2.8 Western blot

After the homogenization, the enhanced tube was taken out and placed on ice for 30 min. Centrifuging the enlarged tube at 12,000 rpm for 20 min at 4 °C. The supernatant was transferred to a fresh EP tube and centrifuged once more to eliminate it. The total protein concentration of the tumor samples was calculated using the concentration and absorbance value of the BSA standard (Sigma, A7906), and the samples were then frozen at -80 °C for subsequent use.

2.9 The percentages of CD8 + T cells and NK cells in local tumor tissues were detected by flow cytometry

Using the tumor tissue dissociation kit, the tumor tissue was trimmed clean, the necrotic tissue, epidermis, fat and other structures were removed, and then rinsed with pre-cooled PBS. 0.1–1 g samples were cut from the central part of the tumor tissue and placed in a disposable sterile Petri dish. Tumor tissue digestive enzymes (RPMI1640 cell medium, 2.35Ml. Enzyme D, 100 µl, enzyme R, 10 µl, and enzyme A, 12.5 µl. After the program was finished, the cell suspension was collected through a 70 µm cell filter screen, centrifuged (300 g, 7 min), and the supernatant was poured out, washed once by adding 2 mL of precooled PBS, and then resuspended in 1 mL of PBS. After cell counting, 2×10^6 cells were taken into the flow tube, and the corresponding antibodies were added. 30 min of incubation at room temperature in the dark were followed by the addition of 2 mL of precooled PBS. After blowing and washing, the cells were centrifuged (350 g, 5 min, 4℃), and the supernatant was poured out. It was resuspended in 500µL of precooled PBS and filtered through a 70 µm screen into a new flow tube for flow cytometry.

2.10 Immunofluorescence staining

The tumor tissues were excised, fixed for two hours in 0.1 M PB solution containing 4% paraformaldehyde, and then transferred to a solution of 25% sucrose to dehydrate for more than twenty-four hours. The necrotic tissue was removed, trimmed and embedded in tissue glue. Sagittal sections with a thickness of 10 µm were prepared along the longitudinal direction by a constant cold box microtome and directly attached to the cation slide. The tissue glue surrounding the specimen was gently flushed with 0.1 M PB before being incubated for 30 min at room temperature with a blocking solution made up of 3% donkey serum, 0.5% Triton X-100, and 0.1 M PB (pH 7.4). Following incubation, rabbit anti-CD11b (Abcam, ab133357, 1:2000) and rat anti-Gr-1 (BioLegend, 108405, 1: 2000) were added drip. 200) at 4° C overnight. The next day, after washing with 0.1 M PB solution, Alexa 488 fluorescein donkey anti-rabbit secondary antibody (Thermo Fisher, A-11034, 1:500) and Alexa 594 fluorescein donkey anti-rat secondary antibody (Thermo Fisher, A-11037, l: 500) and DAPI (1:500000) were added as drops. (containing 0.1 M PB, 0.5% Triton X-100, and 1% donkey serum at a pH of 7.4) were incubated in a wet box for 2 h at room temperature in the dark. After washing with 45 mL of 0.1 M PB, the coverslips were covered by dropping 50% glycerol. The pictures were examined and captured using a microscope.

2.11 The cell trace is far red

Ce1lTrace Far Red (Thermo Fisher, C34564) frozen at -20° C was removed, thawed at room temperature, and dissolved by adding 20µL of DMSO. Centrifuged and resuspended into 3 mL of precooled PBS, the primary T cells obtained from the nylon hair column were incubated for 30 min at room temperature in the dark before being added to 3 µL of DMSO-dissolved CellTrace Far Red dye. After five minutes of darkness and room temperature incubation, 15 mL of 1640 cell media with 10% inactivated FBS was added. The cells were washed by gentle blowing and centrifuged (250 g, 10 min, 4° C). The cells were resuspended in 3 mL of warmed 1640 media (with 10% inactivated FBS) after the supernatant was discarded.

2.12 CD3/CD28 dynabeads

CD3/CD28 Dynabeads (Thermo Fisher, 11131D) stored in a refrigerator at 4 0C were removed, and after vortexing for more than 30 s for resuspension, magnetic beads equal to T cells were removed into I.5 mL EP tubes. 1 mL of T cell isolation buffer was added and Ss was vortexed. The EP tube was put into a DynaMagTM-2 magnetic frame, and the supernatant was discarded after min. 1640 cell medium (containing 10% inactivated fetal bovine serum) equal to the volume of the original magnetic beads was added for time, and then the mixture was mixed by blowing.

2.13 Co-culture of MDSC and T cells

MDSCS were resuspended in 1640 cell medium, which contains 10% inactivated fetal bovine serum, and the cell content was adjusted to 1×10^6 cells/mL from rats in the model group and the combination group. CellTrace Far Red-labeled primary splenic T cells were collected, and their density was increased to 1×10^6 cells per milliliter using 1640 medium with 10% inactivated fetal bovine serum. T cells were co-cultured with MDSCS from the model group and MDSCS from the combination group at a 1: 2 ratio. 100μL of MDSC suspension (1×10^5 cells) and 200 μL of spleen T cell suspension (1×10^5 cells) were mixed and seeded into 24-well cell culture plates. At the same time, T cell culture Wells alone without MDSC cell suspension were set up. The co-culture system was then supplemented with CD3/CD28 immunomagnetic beads corresponding to the amount of T cells, recombinant IL-2 (rIL-2), and recombinant granulocyte–macrophage colony-stimulating factor (rGM-CSF) (final concentrations: 30U/mL and 10 ng/mL, respectively). Only rIL-2 was added in the T cell culture system, and negative control Wells without CD3/CD28 Dynabeads stimulation were set up. Daily replacements of fresh culture medium with rIL-2 (30 U/mL) and rGM-CSF (10 ng/mL) were made while the plates were cultured in a CO_2 incubator.

2.14 Flow cytometry detection of T cell proliferation and activation

After the cells were mixed and blown, they were transferred to a 1.5 mL EP tube and placed in a DynaMagTM-2 magnetic stand for 2 min. The aspirated cell suspension, filtered through a 70 μm screen into a flow tube, centrifuged (350 g, 5 min, 4 ℃), and resuspended in 100μL PBS after removing the supernatant. Coupled with fluorescein BB700 mouse anti-CD3e antibody (BD Biosciences, 553032, 3μL), fluorescein FITC anti-mouse CD4 antibody (Thermo Fisher, 11–0049-42, 3μL) and fluorescein PE mouse anti-CD8a antibody (Thermo Fisher, 12–0088-42, 2.5μL) were added. For 30 min, the cells were incubated at room temperature in the dark. At the end of incubation, 2 mL of PBS was added, blown, washed, centrifuged (350 g, 5 min, 4 ℃), resuspended in 500μL of PBS, and detected by flow cytometry.

2.15 Data and images were processed and statistically analyzed

All measurement data were checked for normality, and those that passed muster were given the mean ± standard error (Means ± SEM) notation. The statistical analysis was performed using SPSS26.0 program. A T test using an independent sample was utilized to compare the two groups. Multiple groups were compared using one-way analysis of variance. Statistics were judged significant at $P < 0.05$. Graphpad Prism7.0 software was used to produce statistical charts, and Adobe Illustrator2020 software was used for processing and formatting.

3 Results

3.1 Albumin-bound paclitaxel combined with Sophora subprostrate polysaccharide inhibits the tumor growth of breast cancer cells and model rats

The cell growth curve for the Sophora subprostrate polysaccharide group showed an increasing growth rate, with no discernible difference in cell growth between the two groups during the first four days. However, starting on day 5, tumor cell proliferation in the Sophora subprostrate polysaccharide group was noticeably slower compared to the untreated control group. By the end of the 7-day experiment, a more pronounced growth difference emerged, with a significant difference between the two groups (Fig. 1A).. In the third week after inoculation of SHZ-88 cells, the tumor bodies of the model group, the Sophora subprostrate polysaccharide group, the paclitaxel group and the combined administration group were taken out for photography and weighing. In comparison to the model group, the tumor weights in the paclitaxel and combination administration groups were lower (Fig. 1B).

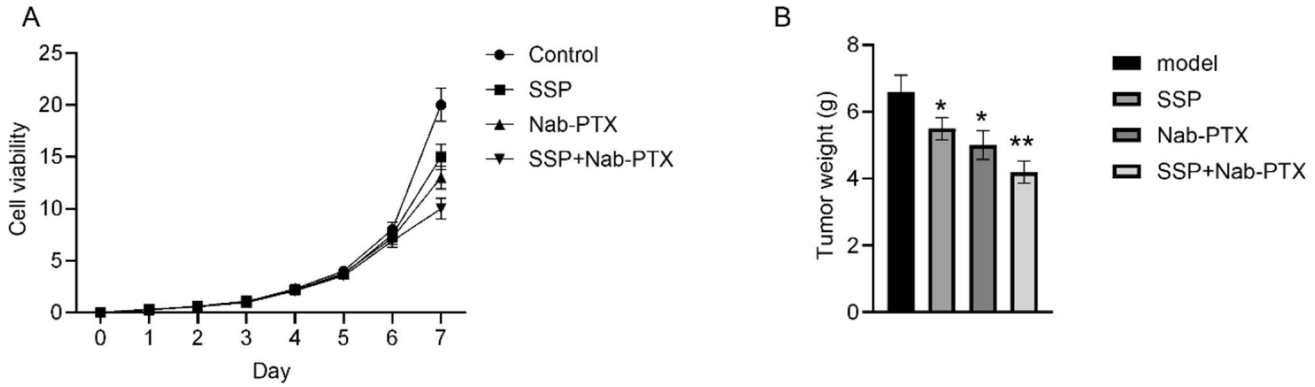

Fig. 1 **A** Growth curves of breast cancer cells after administration of different drugs. **B** Tumor formation weight of breast cancer model rats after drug administration

3.2 The anti-inflammatory effect of albumin-bound paclitaxel combined with Sophora subprostrate polysaccharide on breast cancer model rats

The development of tumor cells and inflammatory cytokines in the tumor microenvironment are closely linked. In the model group, the levels of IL-2 and IFN-γ in local tumor tissue were significantly lower compared to the control group, while IL-6, IL-10, and TGF-β levels were significantly higher. In comparison to the model group, the Sophora subprostrate polysaccharide group, paclitaxel group, and combination group showed significant increases in IL-2 and IFN-γ levels, alongside significant reductions in IL-6, IL-10, and TGF-β levels (Fig. 2A, B). In order to further clarify the effect of albumin-bound paclitaxel combined with Sophora subprostrate polysaccharide on the inflammatory level of the tumor in the breast cancer model rats, each group's rat local tumor tissues were stained. According to the findings, both the model group and the combination administration group had a significant number of lymphocytes with a rounded shape and blue-purple nuclei in the local tumor tissues. There was also a clear inflammatory infiltrate. Rats in the combination treatment group dramatically reduced the infiltration of inflammatory cells in the local tumor tissues as compared to the model group (Fig. 2C).

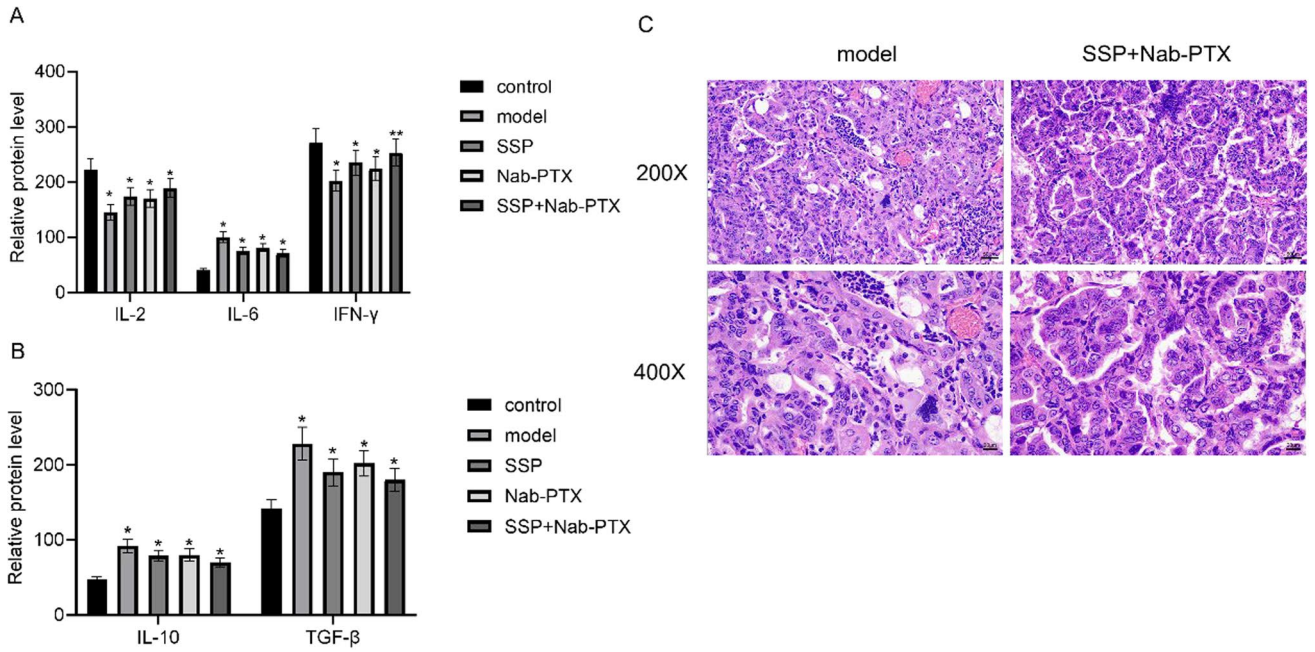

Fig. 2 **A**, **B** Pro- inflammatory and anti-inflammatory factor expression levels in nearby tumor tissues following various medication interventions. **C** HE staining showed the infiltration of inflammatory cells in the local tumor tissues

3.3 To investigate the effect of albumin-bound paclitaxel combined with Sophora subprostrate polysaccharide on anti-tumor immune cells in the tumor tissues of breast cancer model rats

The infiltration of killer immune cells in the local tumor tissue directly marks the strength of anti-tumor immune function. Therefore, the proportion of CD8 + T cells and NK cells in the local tumor tissue was detected to determine whether albumin-bound paclitaxel combined with Sophora subprostrate polysaccharide can enhance the local anti-tumor immune function.

In the single cell suspension of the local tumor tissue from the rats in the model group and the albumin-bound paclitaxel mixed with Sophora subprostrate polysaccharide group, CD3e and CD8a antibodies were utilized to mark the CD8 + T cell population. The ratio of CD8 + T cells in the rats in the combination administration group increased in comparison to the model group (Fig. 3A). CD3e and CD49b antibodies were used to label the NK cell population in the local tumor tissue of rats in the model and combined administration groups, and the proportion of NK cells in the combined administration group was significantly higher than that in the model group (Fig. 3B). Perforin and granzyme are important cytotoxic proteins, which are mainly stored in CD8 + T cells and NK cells. After being secreted into the extracellular space, perforin and granzyme exert cytotoxic effects in a contact dependent manner. To ascertain if albumin-bound paclitaxel mixed with Sophora subprostrate polysaccharide was effective, the expression levels of perforin and granzyme B in local tumor tissues were measured in the current investigation. enhanced CD8 + T cell and NK cell killing capacity in nearby tumor tissues. According to the Figure, when albumin-bound paclitaxel and Sophora subprostrate polysaccharide were combined, the contents of perforin and granzyme B, which were linked to the killing function of anti-tumor immune cells, were significantly higher in the local tumor tissues of the rats than they were in the model group (Fig. 3C). Additionally, the model group's tumor tissues had considerably higher amounts of IgG, IgM, and IgA compared to the control group. The levels of IgG, IgM, and IgA in the Sophora subprostrate polysaccharide group and the combined drug group were significantly lower than those in the model group (Fig. 3D).

3.4 The effect of albumin-bound paclitaxel combined with Sophora subprostrate polysaccharide on immunosuppressive cells in breast cancer model rats

In the single-cell suspension of the local tumor tissues from the model group and the rats receiving combination treatment, CDllb and Gr-1 antibodies were employed to mark the MDSC. The ratio of MDSC in the local tumor tissues of the combined administration rats was considerably lower than that of the model group (Fig. 4A, B). As shown in Fig. 4C, CDLLB-labeled myeloid cells were widely distributed in the local tumor tissues of the model group and the combined administration group, among which MDSC were co-labeled with Gr-1. In comparison to the combined

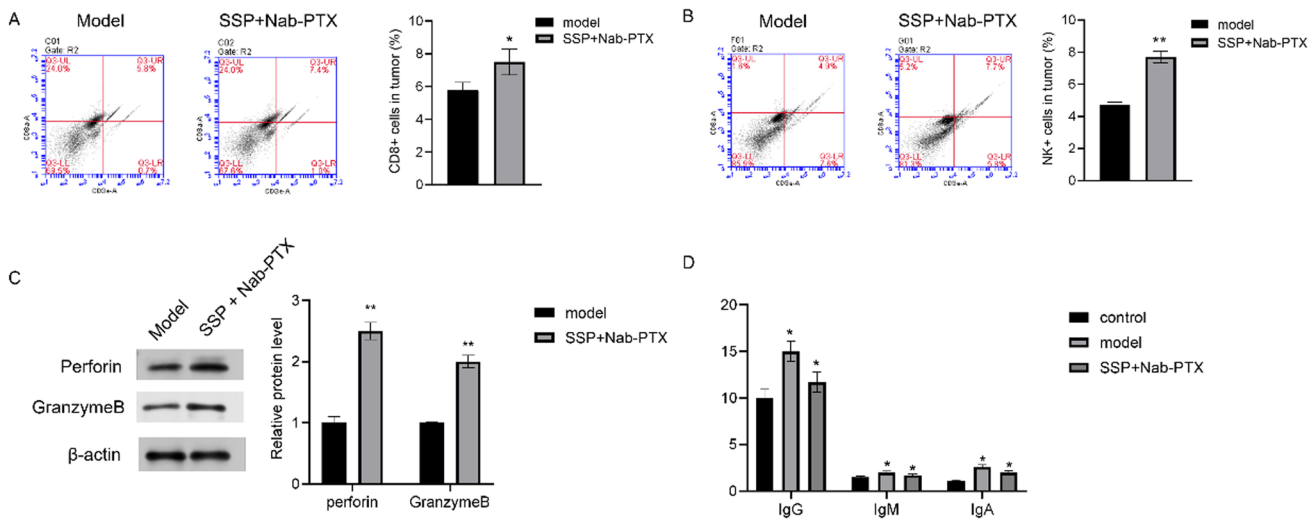

Fig. 3 **A**, **B** Flow-cytometric representation of CD8 + T cells and the percentage of CD8 + T cells. **C** Protein bands and expression levels of perforin and granzyme B in the tumor of each group. **D** Effects of albumin-bound paclitaxel combined with polysaccharides on humoral immune indexes in breast cancer model rats

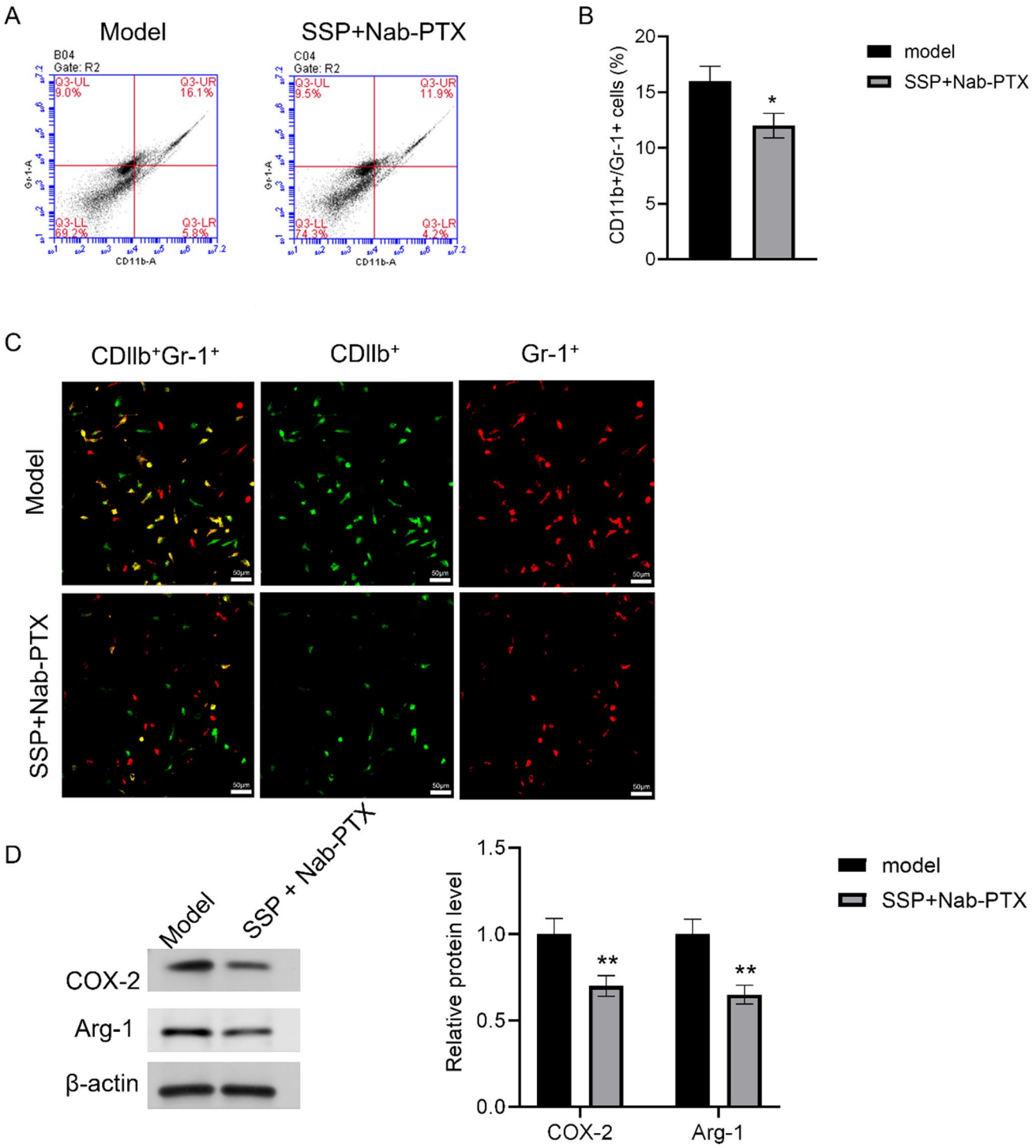

Fig. 4 **A** Representative flow cytometry of MDSC in each group. **B** The proportion of MDSC cells in each group. **C** MDSC (yellow) co-labeled with CDllb (green) and Gr-1 (red) in local tumor tissue. **D** Representative photos of COX-2 and Arg-I protein bands, as well as relative protein expression levels in each group's local tumors of rats

administration group, the model group's distribution of MDSC in the local tumor tissues was noticeably thicker. Cytochrome oxidase subunit 2 (COX-2) and arginase-1 (Arg-1) are important proteins for MDSC to exert inhibitory effects on CD8 + T cells and NK cells. The protein expression levels of COX-2 and Arg-1 in the local tumor tissues of tumor-bearing rats were identified to ascertain the impact of albumin-bound paclitaxel mixed with Sophora subprostrate polysaccharide on the immunosuppressive function of MDSC. When compared to the model group, the

combined group's local tumor tissues had considerably less COX-2 and Arg-1, two molecules linked to the immunosuppressive function of MDSC (Fig. 4D).

3.5 The immunosuppressive effect of albumin-bound paclitaxel combined with Sophora subprostrate polysaccharide on breast cancer model rats

This study performed in vitro experiments to confirm the immunosuppressive impact of albumin-bound paclitaxel coupled with Sophora subprostrate polysaccharide on breast cancer model rats. Normal T cells were co-cultured with MDSC from the combination group and the model group. The immunosuppressive function of MDSC in tumor-bearing rats can be displayed more intuitively.

FarRed dye can enter cells and bind to intracellular proteins; the nucleus shows the staining the most prominently. The dye entering the cell will be distributed equally to the daughter cells during cell division and proliferation, therefore the fluorescence intensity of the dye will decrease as the number of cells increases. The fluorescence intensity of FarRed detected by flow cytometry can effectively reflect the cell proliferation level. The MDSC-T cell co-culture method considerably reduced T cell proliferation compared to T cells cultivated alone, and the inhibitory effect of MDSC on T cell proliferation in the combined treatment group was less pronounced than that in the model group (Figs. 5A and 6A).

IL-2 is an important cytokine that stimulates the activation of T cells. The IL-2 receptor's A chain is the CD25 molecule. After T cells were co-cultured with MDSC of tumor-bearing rats in both the model group and the combination group, the expression of CD25 molecules on the surface of T cells was significantly reduced when compared to T cells cultured alone, while the inhibitory effect of MDSC on T cell activation was weaker in the combination group than in the model group (Figs. 5B and 6B).

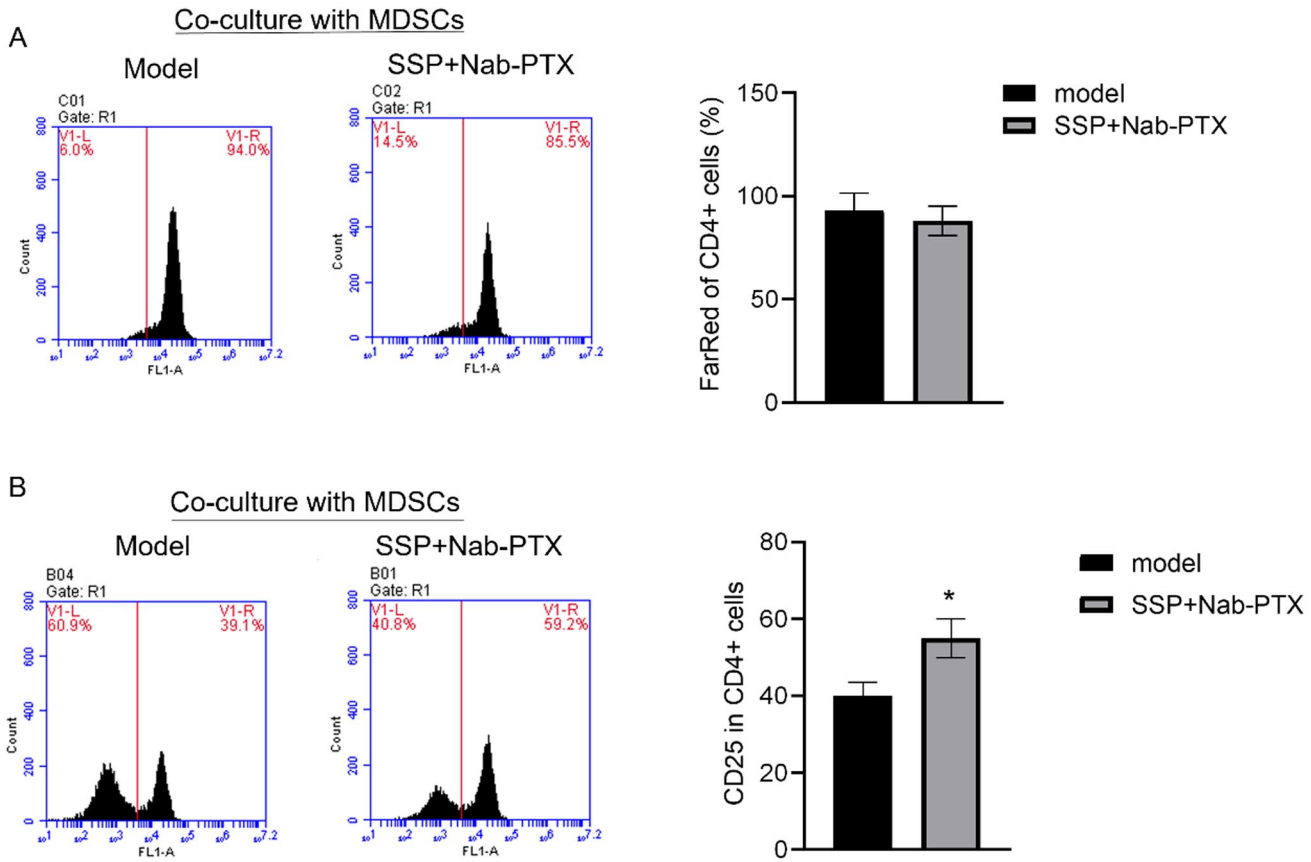

Fig. 5 **A** Flow representative plot of the cellular proliferation level of CD4 + T cells measured by FarRed. **B** CD4 + T cell proliferation in the co-culture system

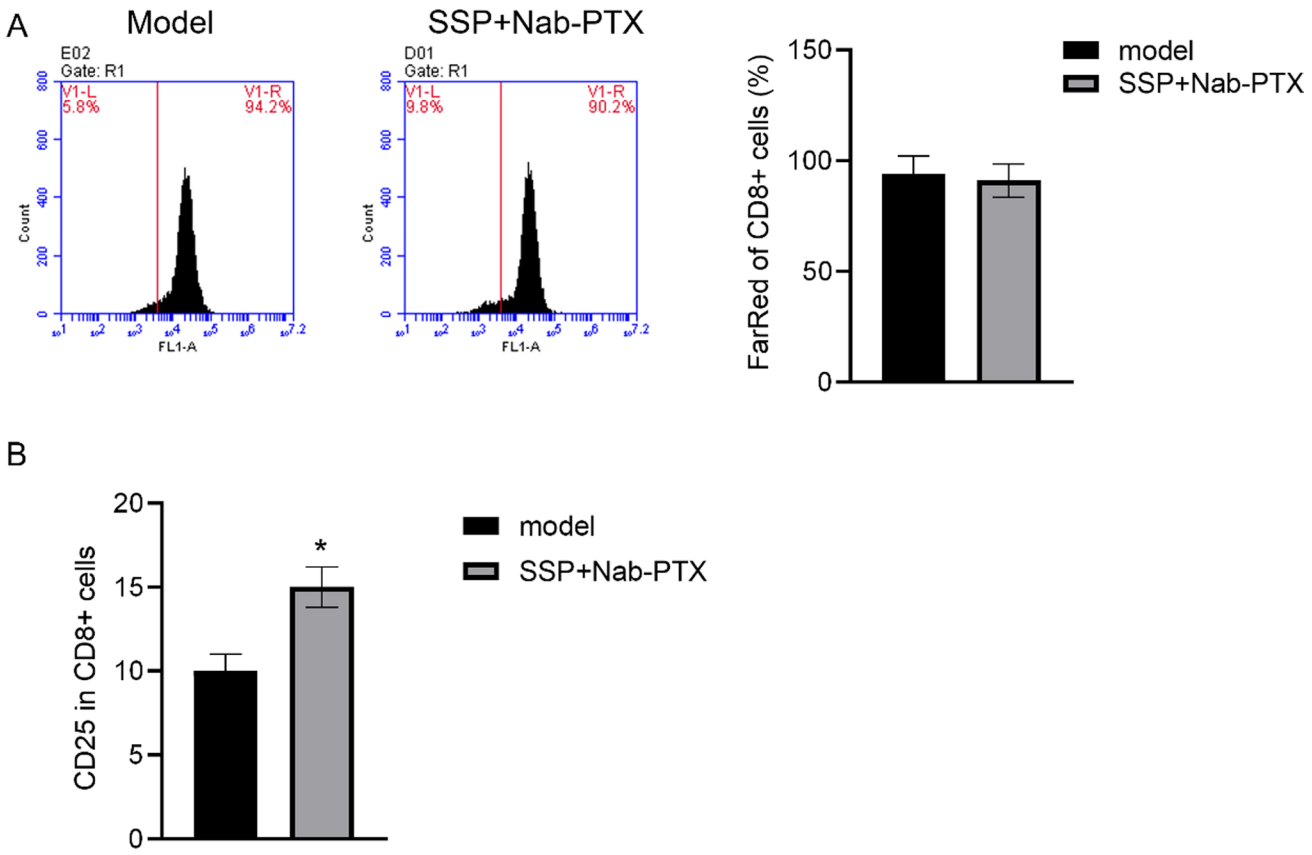

Fig. 6 **A** Flow representative plot of the cellular proliferation level of CD8 + T cells measured by FarRed. **B** CD8 + T cell proliferation in the co-culture system

4 Discussion

The inhibition of inflammation in tumor-bearing bodies has become a critical focus in cancer treatment research. While nonsteroidal anti-inflammatory drugs (NSAIDs) show promise in reducing inflammation, their effective doses in cancer therapy often result in off-target effects and toxicity, limiting their clinical applicability [32]. Tumor progression is driven by a complex network of inflammatory factors, and inflammation promotes tumor development not merely through a single factor but via a multitude of signaling pathways. This study confirmed the systemic and local anti-inflammatory effects of albumin-bound paclitaxel combined with Sophora subprostrate polysaccharide in tumor-bearing rats, through the modulation of inflammatory factors within the tumor microenvironment. These findings suggest a potential integration of acupuncture and related therapies in clinical cancer treatments by regulating these inflammatory pathways [33].

Inflammatory cytokines play a pivotal role in tumor progression and serve as important markers of inflammation. In this study, pro-inflammatory cytokines such as TNF-α and IL-1β, as well as the anti-inflammatory cytokine IL-10, were evaluated in the local tumor tissues of the experimental rats. TNF-α, which is not only produced by tumor cells but also present in the surrounding tumor tissue, is a critical mediator of tumor growth and has been implicated in the pathogenesis of various cancers [34, 35]. It is also known to influence the immune system of the tumor-bearing body by interacting with myeloid-derived suppressor cells (MDSCs), impairing their differentiation and maturation [36]. Additionally, TNF-α stimulates the release of immunosuppressive molecules, such as COX-2 and Arg-1, from MDSCs, which inhibit lymphocyte proliferation and suppress the anti-tumor immune response [37]. In our study, the levels of TNF-α and IL-1β were significantly elevated in the tumor-bearing rats following breast cancer cell injection, while IL-10 levels were also notably higher in the tumor-bearing animals, reflecting a natural compensatory anti-inflammatory response.

The combination therapy led to a reduction in TNF-α and IL-1β levels in the local tumor tissues, suggesting that the treatment might mitigate tumor-induced inflammation. This finding is consistent with studies that show that

acupuncture and related therapies can modulate immune responses by enhancing the activity of NK cells, CD4 + T cells, and CD8 + T cells, while promoting the production of immune effector molecules like interferon-γ [38, 39]. These immune cells play crucial roles in the anti-tumor immune response, and their activation within the tumor microenvironment is vital for combating tumor growth [40, 41].

However, the role of immune cells in the tumor microenvironment requires further investigation. Our results show that the tumor-bearing rats exhibited significant immunosuppression, evidenced by reduced proportions of CD8 + T cells and NK cells, which are essential for the immune system's ability to target and eliminate tumor cells. After treatment, these immune cell populations increased, indicating that the combination therapy alleviates the immunosuppressive state within the tumor microenvironment. Specifically, the perforin-granzyme pathway, a key mechanism for tumor cell destruction by CD8 + T cells and NK cells, was activated, as evidenced by the increased expression of perforin and granzyme B in local tumor tissues [42, 43]. This suggests that the combined treatment not only enhances the immune cell-mediated tumor-killing capacity but also reduces the immunosuppressive influence of MDSCs.

Further supporting this, the treatment reduced the expression of COX-2 and Arg-1 in tumor tissues, which are known to be associated with the immunosuppressive activity of MDSCs [44]. This reduction implies that the combination therapy may reverse the immunosuppressive microenvironment by reducing the inhibitory effects of MDSCs. In vitro co-culture experiments with MDSCs and T cells were also performed, showing similar results, reinforcing the idea that the combined therapy has a direct effect on modulating immune cell activity.

Despite these promising findings, the use of rats as an animal model raises important questions regarding the relevance of these results to human breast cancer. The physiological differences between rats and humans, including variations in immune cell functions and the tumor microenvironment, may limit the direct translation of these results to human patients. Further studies are needed to determine whether the observed effects on immune cell modulation and inflammation in the rat model accurately reflect the complexities of human breast cancer [45, 46]. As such, more research is needed to explore the precise biological mechanisms and immune interactions in human models to validate the therapeutic potential of this combined treatment approach [47, 48].

5 Conclusion

Our study demonstrates that the combination of albumin-bound paclitaxel and Sophora subprostrate polysaccharide (SSP) effectively reduces local inflammation, alleviates immunosuppression, and enhances anti-tumor immune responses, ultimately slowing tumor progression. These findings highlight the potential of integrating immune modulation with chemotherapy as a promising strategy for cancer treatment. For future research, further investigations are needed to elucidate the precise molecular mechanisms underlying the synergy between paclitaxel and SSP, optimize dosage and administration strategies, and evaluate long-term efficacy and safety in preclinical and clinical settings. Clinically, our findings provide a scientific basis for exploring this combination therapy as a complementary approach to existing cancer treatments, particularly in patients with highly immunosuppressive tumor microenvironments.

5.1 Limitations of this study

While our study provides valuable evidence on the synergistic effects of albumin-bound paclitaxel and Sophora subprostrate polysaccharide (SSP) in modulating the tumor microenvironment and enhancing anti-tumor immunity, several limitations should be acknowledged. First, our study was conducted in a tumor-bearing rat model, and the findings may not fully translate to human patients due to species-specific differences in immune responses and tumor microenvironment characteristics. Second, while we observed significant immunomodulatory effects, the precise molecular mechanisms underlying the synergy between paclitaxel and SSP require further investigation, particularly in terms of signaling pathways and tumor-specific immune responses. Third, the study primarily focused on local tumor immune infiltration and systemic immune activation, but potential off-target effects and long-term safety of the combination therapy were not assessed. Finally, clinical validation through well-designed trials is necessary to determine the optimal dosing regimen, treatment duration, and potential interactions with existing cancer therapies. Despite these limitations, our study lays a foundation for future research and clinical applications, emphasizing the need for further preclinical and clinical investigations to fully assess the therapeutic potential of this combination strategy.

Author contributions Changli Ding and Zhuolin Li contributed equally to this work as co-first authors. Changli Ding was responsible for the conceptualization and experimental design of the study. Zhuolin Li carried out the data acquisition and performed statistical analyses. Ying Zheng participated in the experimental procedures and contributed to the interpretation of the results. Kaichun Li and Wenyan Yu assisted in data collection and performed technical support in key assays. Lingzhijie Kong was involved in manuscript preparation and figure development. Zhiyong Zhang supervised the study, provided critical revisions, and approved the final manuscript as the corresponding author. All authors reviewed and approved the final manuscript.

Funding This study was supported by the Scientific research project of the Discipline Boost Program of Shanghai Fourth People's Hospital. Project number: SY-XKZT-2020-1020.

Data availability The datasets generated and analyzed during the current study are available from the corresponding author on reasonable request.

Declarations

Ethics approval and consent to participate All experimental procedures involving animals were conducted in accordance with the guidelines of the Institutional Animal Care and Use Committee (IACUC) of Shanghai Fourth People's Hospital affiliated to Tongji University. The study protocol was reviewed and approved by the committee. All efforts were made to minimize animal suffering and reduce the number of animals used in the study.

Consent for publication Not applicable.

Competing interests The authors declare no competing interests.

Open Access This article is licensed under a Creative Commons Attribution-NonCommercial-NoDerivatives 4.0 International License, which permits any non-commercial use, sharing, distribution and reproduction in any medium or format, as long as you give appropriate credit to the original author(s) and the source, provide a link to the Creative Commons licence, and indicate if you modified the licensed material. You do not have permission under this licence to share adapted material derived from this article or parts of it. The images or other third party material in this article are included in the article's Creative Commons licence, unless indicated otherwise in a credit line to the material. If material is not included in the article's Creative Commons licence and your intended use is not permitted by statutory regulation or exceeds the permitted use, you will need to obtain permission directly from the copyright holder. To view a copy of this licence, visit http://creativecommons.org/licenses/by-nc-nd/4.0/.

References

1. Sung H, et al. Global cancer statistics 2020: GLOBOCAN estimates of incidence and mortality worldwide for 36 cancers in 185 countries. CA Cancer J Clin. 2021;71(3):209–49.
2. Davis NM, et al. Deregulation of the EGFR/PI3K/PTEN/Akt/mTORC1 pathway in breast cancer: possibilities for therapeutic intervention. Oncotarget. 2014;5(13):4603–50.
3. Tobias DK, et al. Markers of inflammation and incident breast cancer risk in the women's health study. Am J Epidemiol. 2018;187(4):705–16.
4. Zaalberg A, et al. Chronic inflammation promotes skin carcinogenesis in cancer-prone discoid lupus erythematosus. J Invest Dermatol. 2019;139(1):62–70.
5. Tu T, Buhler S, Bartenschlager R. Chronic viral hepatitis and its association with liver cancer. Biol Chem. 2017;398(8):817–37.
6. Greten FR, Grivennikov SI. Inflammation and cancer: triggers, mechanisms, and consequences. Immunity. 2019;51(1):27–41.
7. Jang JH, et al. Breast cancer cell-derived soluble CD44 promotes tumor progression by triggering macrophage IL1beta production. Cancer Res. 2020;80(6):1342–56.
8. Derin D, et al. Serum levels of apoptosis biomarkers, survivin and TNF-alpha in nonsmall cell lung cancer. Lung Cancer. 2008;59(2):240–5.
9. Ma Y, et al. IL-6, IL-8 and TNF-alpha levels correlate with disease stage in breast cancer patients. Adv Clin Exp Med. 2017;26(3):421–6.
10. Fox P, et al. Markers of systemic inflammation predict survival in patients with advanced renal cell cancer. Br J Cancer. 2013;109(1):147–53.
11. Andersen BL, et al. Cells, cytokines, chemokines, and cancer stress: a biobehavioral study of patients with chronic lymphocytic leukemia. Cancer. 2018;124(15):3240–8.
12. Mitsunaga S, et al. Serum levels of IL-6 and IL-1beta can predict the efficacy of gemcitabine in patients with advanced pancreatic cancer. Br J Cancer. 2013;108(10):2063–9.
13. Nakamura K, Smyth MJ. Targeting cancer-related inflammation in the era of immunotherapy. Immunol Cell Biol. 2017;95(4):325–32.
14. Bruchard M, et al. Chemotherapy-triggered cathepsin B release in myeloid-derived suppressor cells activates the Nlrp3 inflammasome and promotes tumor growth. Nat Med. 2013;19(1):57–64.
15. Molon B, et al. Chemokine nitration prevents intratumoral infiltration of antigen-specific T cells. J Exp Med. 2011;208(10):1949–62.
16. Low JT, et al. Transplantable programmed death ligand 1 expressing gastroids from gastric cancer prone Nfkb1(-/-) mice. Cell Death Dis. 2021;12(12):1091.
17. Burkitt MD, et al. Signaling mediated by the NF-kappaB sub-units NF-kappaB1, NF-kappaB2 and c-Rel differentially regulate Helicobacter felis-induced gastric carcinogenesis in C57BL/6 mice. Oncogene. 2013;32(50):5563–73.
18. Roca H, et al. Apoptosis-induced CXCL5 accelerates inflammation and growth of prostate tumor metastases in bone. J Clin Invest. 2018;128(1):248–66.

19. Hanson EM, et al. Myeloid-derived suppressor cells down-regulate L-selectin expression on CD4+ and CD8+ T cells. J Immunol. 2009;183(2):937–44.
20. Velazquez-Caldelas TE, et al. Unveiling the link between inflammation and adaptive immunity in breast cancer. Front Immunol. 2019;10:56.
21. Kanterman J, Sade-Feldman M, Baniyash M. New insights into chronic inflammation-induced immunosuppression. Semin Cancer Biol. 2012;22(4):307–18.
22. Ku AW, et al. Tumor-induced MDSC act via remote control to inhibit L-selectin-dependent adaptive immunity in lymph nodes. Elife. 2016. https://doi.org/10.7554/eLife.17375.
23. Srivastava MK, et al. Myeloid-derived suppressor cells inhibit T-cell activation by depleting cystine and cysteine. Cancer Res. 2010;70(1):68–77.
24. Veglia F, Sanseviero E, Gabrilovich DI. Myeloid-derived suppressor cells in the era of increasing myeloid cell diversity. Nat Rev Immunol. 2021;21(8):485–98.
25. Stiff A, et al. Nitric oxide production by myeloid-derived suppressor cells plays a role in impairing fc receptor-mediated natural killer cell function. Clin Cancer Res. 2018;24(8):1891–904.
26. Idorn M, et al. Correlation between frequencies of blood monocytic myeloid-derived suppressor cells, regulatory T cells and negative prognostic markers in patients with castration-resistant metastatic prostate cancer. Cancer Immunol Immunother. 2014;63(11):1177–87.
27. Lu C, et al. Current perspectives on the immunosuppressive tumor microenvironment in hepatocellular carcinoma: challenges and opportunities. Mol Cancer. 2019;18(1):130.
28. Alshetaiwi H, et al. Defining the emergence of myeloid-derived suppressor cells in breast cancer using single-cell transcriptomics. Sci Immunol. 2020. https://doi.org/10.1126/sciimmunol.aay6017.
29. LauretMarieJoseph E, et al. Immunoregulation and clinical implications of ANGPT2/TIE2(+) M-MDSC signature in non-small cell lung cancer. Cancer Immunol Res. 2020;8(2):268–79.
30. Friis S, et al. Low-dose aspirin or nonsteroidal anti-inflammatory drug use and colorectal cancer risk: a population-based case-control study. Ann Intern Med. 2015;163(5):347–55.
31. Trabert B, et al. Aspirin, nonaspirin nonsteroidal anti-inflammatory drug, and acetaminophen use and risk of invasive epithelial ovarian cancer: a pooled analysis in the Ovarian Cancer Association Consortium. J Natl Cancer Inst. 2014;106(2):djt431.
32. Gurpinar E, Grizzle WE, Piazza GA. NSAIDs inhibit tumorigenesis, but how? Clin Cancer Res. 2014;20(5):1104–13.
33. Dondossola E, et al. Self-targeting of TNF-releasing cancer cells in preclinical models of primary and metastatic tumors. Proc Natl Acad Sci U S A. 2016;113(8):2223–8.
34. Behboodi N, et al. Association of a variant in the tumor necrosis factor alpha gene with risk of cervical cancer. Mol Biol Rep. 2021;48(2):1433–7.
35. Arancibia R, et al. Tumor necrosis factor-alpha inhibits transforming growth factor-beta-stimulated myofibroblastic differentiation and extracellular matrix production in human gingival fibroblasts. J Periodontol. 2013;84(5):683–93.
36. Qu Y, et al. The effects of TNF-alpha/TNFR2 in regulatory T cells on the microenvironment and progression of gastric cancer. Int J Cancer. 2022;150(8):1373–91.
37. Jong MS, Hwang SJ, Chen FP. Effects of electro-acupuncture on serum cytokine level and peripheral blood lymphocyte subpopulation at immune-related and non-immune-related points. Acupunct Electrother Res. 2006;31(1–2):45–59.
38. Hideaki W, et al. Effect of 100 Hz electroacupuncture on salivary immunoglobulin A and the autonomic nervous system. Acupunct Med. 2015;33(6):451–6.
39. Yuliatun L, et al. Electro-acupuncture therapy increases serum interferon-gamma levels in rats with 7, 12 Dimethylbenz(alpha)anthracene (DMBA)-induced breast tumors. Asian Pac J Cancer Prev. 2017;18(5):1323–8.
40. Zhang Q, et al. Landscape and dynamics of single immune cells in hepatocellular carcinoma. Cell. 2019;179(4):829-845.e20.
41. Li Y, et al. The role of RNA methylation in tumor immunity and its potential in immunotherapy. Mol Cancer. 2024;23(1):130.
42. Huang Z, et al. Electroacupuncture regulates the DREAM/NF-kappaB signalling pathway and ameliorates cyclophosphamide-induced immunosuppression in mice. Acupunct Med. 2019;37(5):292–300.
43. Benmebarek MR, et al. Killing mechanisms of chimeric antigen receptor (CAR) T cells. Int J Mol Sci. 2019;20(6):1283.
44. Yan G, et al. A RIPK3-PGE(2) circuit mediates myeloid-derived suppressor cell-potentiated colorectal carcinogenesis. Cancer Res. 2018;78(19):5586–99.
45. Xu Y, et al. Activated hepatic stellate cells promote liver cancer by induction of myeloid-derived suppressor cells through cyclooxygenase-2. Oncotarget. 2016;7(8):8866–78.
46. Jahan F, et al. Bainbridge SA. A comparison of rat models that best mimic immune-driven preeclampsia in humans. Front Endocrinol. 2023;14:1219205.
47. Abdolahi S, et al. Patient-derived xenograft (PDX) models, applications and challenges in cancer research. J Transl Med. 2022;20(1):206.
48. Ooi SL, et al. Evidence-based review of BioBran/MGN-3 arabinoxylan compound as a complementary therapy for conventional cancer treatment. Integr Cancer Ther. 2018;17(2):165–78.

Publisher's Note Springer Nature remains neutral with regard to jurisdictional claims in published maps and institutional affiliations.